The topological structure of 2D disordered cellular systems

H.M. Ohlenbusch, T. Aste[a], B. Dubertret, and N. Rivier

Équipe de Physique Statistique, LDFC, Université Louis Pasteur, 3 rue de l'Université, 67084 Strasbourg, France

Abstract. We analyze the structure of two dimensional disordered cellular systems generated by extensive computer simulations. These cellular structures are studied as topological trees rooted on a central cell or as closed shells arranged concentrically around a germ cell. We single out the most significant parameters that characterize statistically the organization of these patterns. Universality and specificity in disordered cellular structures are discussed.

PACS. 82.70.Rr Aerosols and foams – 02.50.-r Probability theory, stochastic processes, and statistics – 05.70.Ln Nonequilibrium thermodynamics, irreversible processes

1 Introduction

Cellular structures, space-filling disordered patterns, are widespread in nature [1–3]. In an ordered structure, one must constrain the elementary bricks (or group of them) to satisfy the local rotational symmetry compatible with translational invariance. By contrast, a disordered structure is free of any local symmetry constraint, and only subjected to the inescapable, topological condition of partitioning space. In two dimensions, these structures (froths) are partitions of the plane by irregular polygons. Disorder, or absence of symmetry, imposes minimal incidence numbers (3 edges incident on a vertex, 2 faces incident on a edge). The Four-Corner boundary between the States of Arizona, Utah, Colorado and New Mexico is a decision made in Washington; it has nothing to do with population dynamics or with agricultural efficiency. It is neither topologically, nor structurally stable: a small deformation splits it into two topologically stable three-State vertices, found everywhere else on Earth.

The set of all the possible configurations of a froth can be explored by elementary, local topological transformations [4] which, in two dimensions, are: T1, exchange of neighbours (for example, a flip between the stable alternatives of UT-NM or of AZ-CO as neighbours, about the unstable four-corner boundary); T2, disappearance (or apparition) of a triangular cell into a single vertex. Two alternative, equivalent transformations are the cell-division (called mitosis in biology) and cell-coalescence. It can be easily seen (Fig. 1) that local, specific combinations of division and coalescence generate the two elementary transformation T1 and T2, and *vice versa*. These elementary, local topological transformations are observed in all natural foams, soap froths, metallurgical grain aggregates, but

also in biological tissues (epidermis) [5] or in the cellular networks produced by Bénard-Marangoni convection, whether in the laboratory or on the surface of the sun (solar granulation) [2,3].

In infinite two dimensional (2D) Euclidean froths (or froths with periodic boundary conditions), the average number of neighbours per cell is fixed by the Euler relation to be equal to 6 [2]. Given a cell with n edges, the quantity $q = 6 - n$ is called its topological charge. The sum of the charges of the cells over the whole infinite Euclidean froth must be equal to zero. The topological charge cannot be generated or destroyed. It is just shuffled in between cells by the topological transformations.

In this paper, extensive computer simulation are performed to obtain disordered systems with more than 10^5 cells generated from an hexagonal lattice and applying at random either only T1, or T1 and T2, or cell-division and coalescence transformations. In these simulated froths, we forbid configurations with cells which are neighbours of themselves and cells with two edges. The typical resulting structures are shown in Figure 2.

The structural organization of these computer-generated froths are studied in terms of the relative distances between cells. Two different topological distances can be introduced: the *bond distance* [6,7] and the *shell distance* [8–11] (Sect. 2). These two distances are different: the bond distance is defined on the graph of the froth; the shell distance is best defined on its dual triangulation. They are associated with the number of edges (or vertices) of the shortest paths between two cells. The relation between the two distances is very complex and strongly dependent on the froth organization, because they involve minimal paths.

The characterization of a disordered structure is a difficult task. The absence of translational order or repetitive local configuration makes in principle necessary to
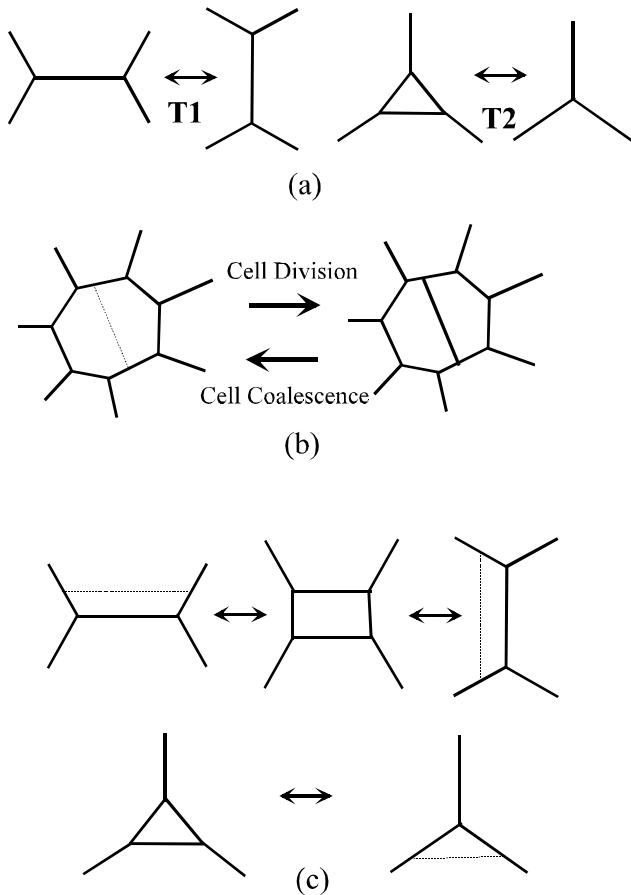
a e-mail: `tomaso,nick@ldfc.u-strasbg.fr`

Fig. 1. A froth is a cellular network generated or transformed by successive applications of two local elementary transformations: T1 (neighbours exchange), and T2 (triangular) cell disappearance (a). These two transformations can also be regarded as combinations (c) of cell division and cell coalescence (b).
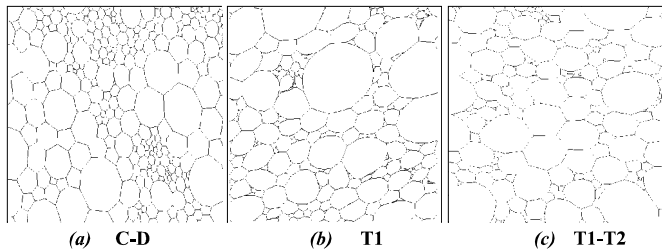

Fig. 3. (a) The forest of n bond trees. (b) In a tree, any vertex at distance t is connected with one bond to a vertex at distance $t-1$. Two of the three cells incident on a vertex at distance t are also incident on a vertex at distance $t-1$. The mean vertex connectivity (z_t) tends asymptotically to 2, which is typical of a tree structure spanning vertices distributed uniformly (see also Fig. 12). In (c) vertices with connectivity $z = 1$ and $z = 3$ are labelled with white and black circles respectively.

Fig. 2. Typical topological froths generated by: (a) Cell division and coalescence; (b) T1 transformations only; (c) T1 and T2 transformations.

know the position, size and shape of every cell in order to completely characterize the structure. But, disorder makes most of this detailed local information unimportant. The physical properties of the froth must be describable in terms of macroscopic statistical information. A simple and powerful way to study disordered cellular systems, is to analyze the structure as organized around a given arbitr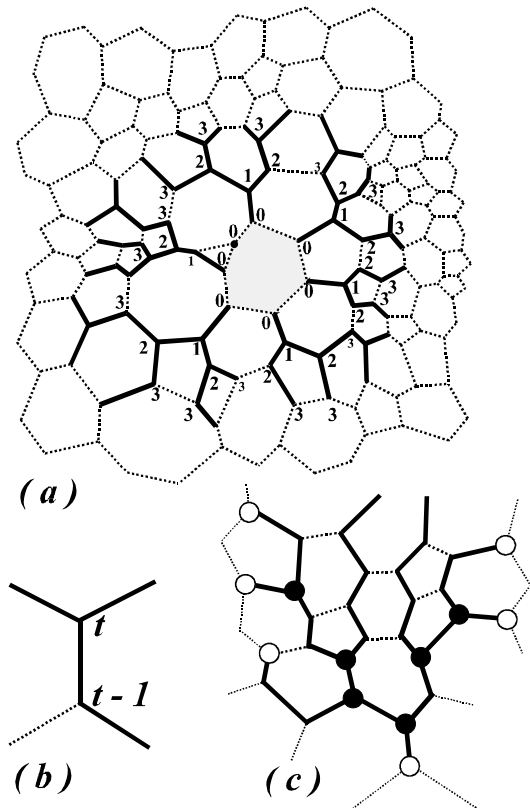ary central cell. The information about the structure can be obtained in terms of the properties of the set of cells at a given distance (bond or shell) from the central cell. We show that the classification by bond distances reduces the froth to a set of trees rooted on the vertices of an arbitrary central cell (see Fig. 3). On the other hand, in terms of shell distance, the froth can be seen as a set of closed layers of cells arranged concentrically around the central cell (see Fig. 4). This classification in terms of distances naturally introduces a structure and a hierarchy in the froth. Moreover, a physical meaning is directly associated to the sets of equally-distant cells: any perturbation, signal or information propagates from a given cell to the whole froth through these structures and cells at the same distance are those reached — on average — at the same time and with equal intensity by the signal. They are the successive wave fronts of the signal in the froth.
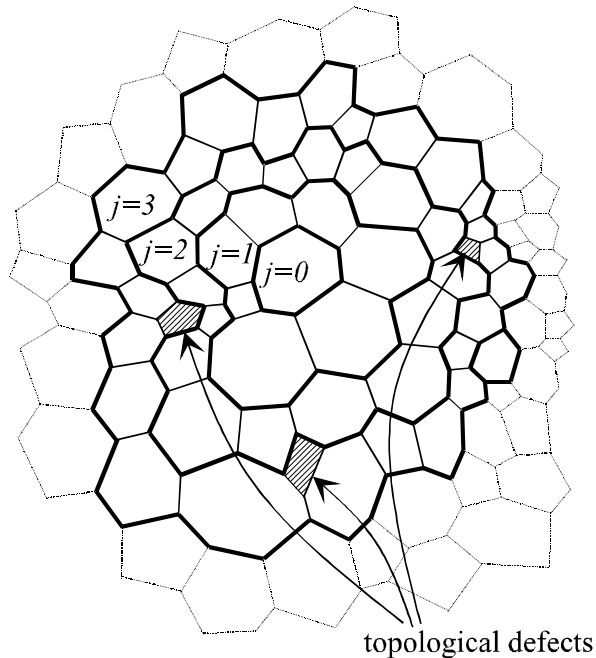
Fig. 4. The shell structure. Any froth can be analyzed as structured in a system of closed concentric layers of cells at the same shell distance with respect to the central cell. The cells (hatched in the figure) in layer (j) with neighbours in layers ($j-1$) and (j) only, are local topological defects included between the layers.

2 Topological structure of a froth

2.1 Topological distances

Consider two cells in a froth. These cells are connected by many paths along the edges of the direct graph or of its dual triangulation. Two different topological distances can be associated with minimal paths:

The bond distance, is the minimum number of edges necessary to connect two cells in the direct graph of the froth[1]. (The concepts of bond distance and of bond neighbours was first introduced by one of the authors [6], who called them T1 distance and T1 neighbours, respectively [7].)

The shell distance (or simply, topological distance [11]), is the minimum number of edges connecting the centers of two cells in the dual triangulation[2].
All the cells in the froth can be classified in terms of distances (bond & shell) with respect to a given "central" cell.

We denote by F_t the number of cells which are at a bond distance t and by K_j the number of cells which are

---

[1] This path is a set of adjacent edges (*'bonds'*) connecting the two cells.

[2] The set of equidistant cells makes a closed layer around the central cell, and successive layers form concentric rings. The edges separating two successive layers form a closed loop: the *'shell'* [11].

at a shell distance j from a given central cell. These quantities are in general dependent on the number of edges n of the central cell. For any froth on the Euclidean plane, F_t and K_j increase with the respective distances. But the rates of growth are characteristics of a specific cellular system and are good, sensitive quantities to characterize its disorder (see Sect. 4 and Refs. [12,13]).

2.2 The n rooted bond trees

Associated with the bond distance, there is a spanning forest of n trees rooted on the central cell and reaching every vertex of the froth in the least number of steps. These trees are the minimal bond paths which join the vertices of the froth with the central cell. Consider a vertex of the froth at a large bond distance t. It has 3 neighbouring vertices, with at least one at a distance $t-1$. Select one of them and connect it with a *bond*. The other neighbouring vertex at $t-1$ (if there is one) is left unconnected. Continue down in distances until a vertex of the central cell is reached. This is the *root* of the tree, which, at this stage, is simply a branch (chain) of t bonds. Then, begin again with another vertex at distance t, down in distances. This second t-branch either meets the first at some point, or it reaches another root (vertex of the central cell). Proceed successively with every vertex at distance t, down in distances until the branch connects another branch or is rooted into the central cell. Consider then the vertices at distance $t-1$ which have not yet been reached by the branches already constructed, and repeat the operations above. By repeating the process to all the vertices yet unspanned at distances t, $t-1$, $t-2$,..., 2, 1, 0, we generate a forest of n trees, where n is the number of vertices (and of edges) of the central cell. These trees are rooted on the central cell and span all the vertices of the froth. Figure 3a shows a forest of trees up to distance 3. Each vertex in the tree has connectivity $2 \leq z \leq 3$, except the root and branch ends which have connectivity 1 (zero if the tree consists of its root vertex only, as happens, for example, if the central cell has a 3-cell as topological neighbour). Call z_t the average vertex connectivity at distance t ($1 \leq z_t \leq 3$ for $t > 0$ and $0 \leq z_0 \leq 1$). It follows immediately that $V_{t+1} = (z_t - 1)V_t$ and $V_1 = z_0 V_0 = z_0 n$. The number of vertices at distance $t > 1$ is therefore related to the number of edges of the central cell (n)

$$V_t = \left[z_0 \prod_{i=1}^{t-1} (z_i - 1) \right] n. \tag{1}$$

The bond distance associated to a cell is the bond distance of its vertex nearest to the central cell. Consider a vertex at distance t. It has 3 incident cells. Two must also be incident on a vertex at distance $t - 1$ (they are separated by the bond linking vertex t to vertex $t - 1$, see Fig. 3b). Therefore, to each vertex at a given distance, there corresponds no more than one cell at the same distance, *i.e.* $F_t = \nu_t V_t$ with $\nu_t \leq 1$. In 2D Euclidean froths, a cell has 6 vertices on average, and 3 cells are incident on any vertex. Therefore we expect $\nu \simeq 0.5$ on average.

A special case is the hexagonal lattice where there are 6 vertices and 6 cells at distance $t = 1$, 12 vertices and 6 cells at $t = 2$, 12 vertices and 12 cells at $t = 3$, and, in general $V_t = F_t = 3(t+1)$ for t odd and $V_t = 3(t+2)$ and $F_t = 6$ for t even. We have therefore $\nu_t = 0.5$ on average, with $\nu_t = 1$ when t is odd and $\nu_t = 0$ when t is even. This difference between even and odd distances is characteristic of the hexagonal lattice. When the froth is disordered, this difference between even and odd distances disappears and, asymptotically, the quantities V_t and F_t grow linearly with the distance t with $\nu_t \simeq 0.5$. The growth law depends on the specific system and it is studied in Sections 3 and 4.

2.3 The shell structure

The structure associated with the shell distance for a typical froth is shown in Figure 4. The shell distance foliates the froth into successive layers of cells surrounding the central cell. Most cells at a (shell) distance j from the central cell have neighbours at distances $j-1$, j and $j+1$. They belong to layer (j). In addition, some cells at distance j (hatched in Fig. 4) have neighbours at distances $j-1$ and j only. These cells are local *defect* inclusions, intercalated between layers $(j-1)$ and (j).

In this paper we characterize the shell structure by the number of cells at distance j, $K_j(n)$, averaged over all n-sided central cells. In the perfect honeycomb (hexagonal froth), $K_j = 6j$, there are no defects, and the successive layers have an hexagonal shape. In a random froth, the layers are roughly circular, but wiggly. At large distances, $K_j(n)$ is larger than for the honeycomb, but still increases linearly with the distance. The rate of increase is related to the degree of disorder and to the number of topological defects in the system [12].

2.4 The combined structure

The quantities F_t and K_j are both radial properties with the angular dependence averaged out. In order to extract information on the angular fluctuations, it is interesting to study the interplay between bond and shell structures. A bond tree develops radially outward from the central cell along edges which are perpendicular to the shells and it broadens sideways along edges parallel to the shells. The distribution in the bond tree of edges parallel to the shells gives therefore a measure of its spread. Call $N(j,t)$ the number of couples of cells that are simultaneously at a shell distance j and at a bond distance t from each other. (Clearly, $\sum_t N(j,t) = K_j N$ and $\sum_j N(j,t) = F_t N$, with N the total number of cells in the system.)

To calculate $N(j,t)$, let one of the cells be the central cell. The other cell is at shell distance j. What is the bond distance t between the two cells? It is readily seen (Fig. 5) that at least 2 bonds are necessary to go from one layer to the next. Thus, $t_{\min} = 2j - 3 = t_R$ for $j \geq 2$. Therefore, t_R is the radial component of the bond distance. (In an hexagonal froth, $t = t_R$, for $j \geq 2$.)
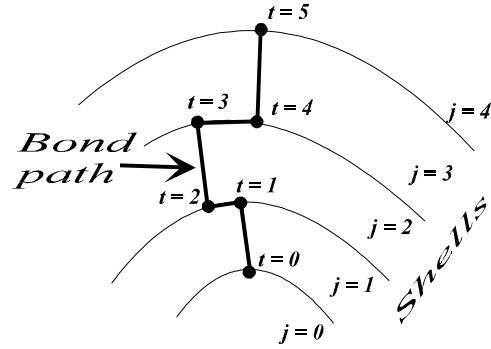

Fig. 5. The shortest bond path crosses at least $t_{\min} = 2j - 3$ vertices to connect the central cell with a cell in the layer j.

In disordered froths, the bond distance t is, in general, much larger than t_R. Suppose, for instance, that a path takes in average $\langle v \rangle$ extra bonds from one layer to the next. These extra bonds correspond to segments of the bond tree parallel to the shell and also to extra vertices associated to the topological defects between the shells. From the central cell to a cell at distance j, there are $\langle v \rangle (j-1)$ additional bonds and the total bond distance is therefore $t = t_R + \langle v \rangle (j-1) = (2+\langle v \rangle)j - 3 - \langle v \rangle$. The number v of extra bonds between layers is a random variable with probability distribution $w(v)$ and mean $\langle v \rangle$. When $w(v)$ is Poissonian, the conditional probability $P(t|j)$ of finding a cell at a bond distance t, given that it lies at a shell distance j, is a shifted Poissonian with average $\bar{t} = \langle v \rangle (j-1) + 2j - 3$ and variance $\sigma^2 = \langle v \rangle (j-1)$ (see Appendix A). The number of couples of cells which are simultaneously at a shell distance j and at a bond distance t is therefore

$$N(j,t) = N K_j P(t|j)$$
$$= N K_j \frac{e^{-\langle v \rangle (j-1)}[\langle v \rangle (j-1)]^{t-2j+3}}{(t-2j+3)!}. \quad (2)$$

The arrangement of the cells in any layer can therefore be described in terms of a single parameter $\langle v \rangle$ only.

3 Simulation of disordered cellular systems

3.1 Coalescence and Division (C-D simulation)

The disordered cellular system is generated staring form an hexagonal lattice of $N_0 = 144\,400$ cells, with periodic boundary conditions, and performing $5N_0$ of T1 transformations on edges chosen at random. Then, a cell, chosen at random, is divided in two parts (mitosis) if it has more than 6 sides or fused by coalescence with one of its neighbours if has less than 6 sides. If it has six sides, it is divided with probability $p_d = 1/4$ or left unchanged with probability $1 - p_d = 3/4$. The coalescence is performed between the cell and one of its neighbours chosen at random. We chose a symmetric mode of division: the two "daughters" of an n-sided "mother" cell have both $2 + n/2$ edges for n
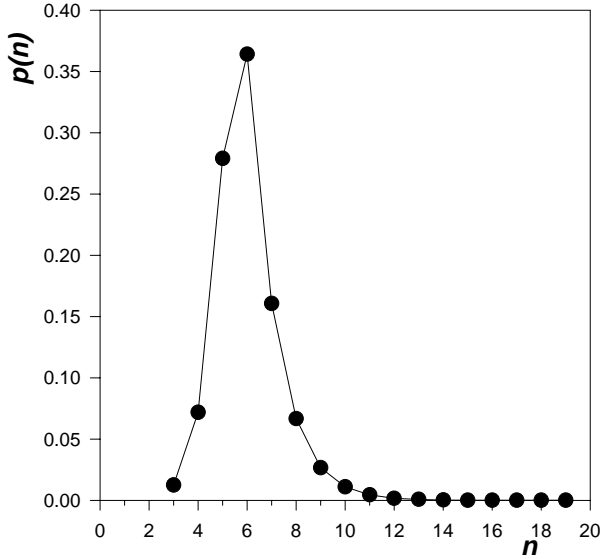
Fig. 6. Distribution of the number of edges per cell in the froth generated by applying cell-division and coalescence transformations (C-D simulation).

Fig. 7. Second moment of the edges distribution (μ_2) *versus* the number of elementary topological transformations, in the system generated by cell-division and coalescence transformations (C-D simulation). The system converges toward a steady state which is independent of the starting configuration. If the simulation starts from a very disordered state, the system self organizes reducing the disorder by random local transformations.

even, and $2 + (n+1)/2$ and $2 + (n-1)/2$ edges if n is odd (which one has which is assigned at random).

After iterating the coalescence-division operations for $10N_0$ times, the resulting structure (shown in Fig. 2a) reaches a stationary number of $N = 114\,475$ cells. The normalized distribution of the number of edges per cell ($p(n)$) is shown in Figure 6. It has a maximum at $n = 6$ and decreases exponentially for $n \geq 6$) as $p(n) = p_6 \exp[-\alpha(n - 6)]$ with $p_6 = 0.37$ and $\alpha = 0.9$. The second moment of the distribution is $\mu_2 = 1.77$, and the Aboav-Weaire parameter [2,14,15] is $a = 0.64$.

This distribution is stationary under further division-coalescence transformations. It is also independent of the initial configuration. We have obtained statistically identical froths starting from the hexagonal lattice ($\mu_2 = 0$) or from a very disordered froth with $\mu_2 > 10$. In the first case, the system evolves from order to disorder during the simulation. By contrast, in the second case, the disorder of the system decreases throughout the simulation (see Fig. 7). This is an example of self organization induced by local random transformations only. The distribution $p(n)$ reaches a steady state, regardless of the parameter p_d which controls the fate of 6-sided cells. However, the number of cells is very sensitive to p_d. For $p_\mathrm{d} = 1/4$, once the steady state is reached, the number of cells in the froth remains also stable. But, when $p_\mathrm{d} = 0$, the number of cells in the system decreases, whereas, when $p_\mathrm{d} = 1/2$, it increases.

3.2 Random T1 (T1 simulation)

An hexagonal lattice of $N = 100\,172$ cells and periodic boundary conditions is disordered by flipping (T1 transformation) $10N$ edges chosen at random. (Note that the T1 transformation conserves the total number of cells in
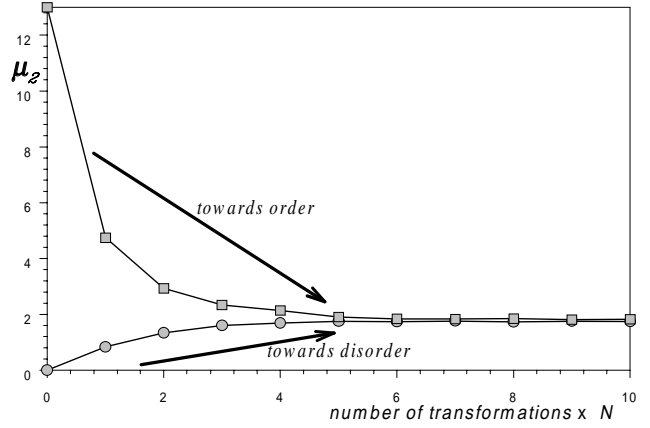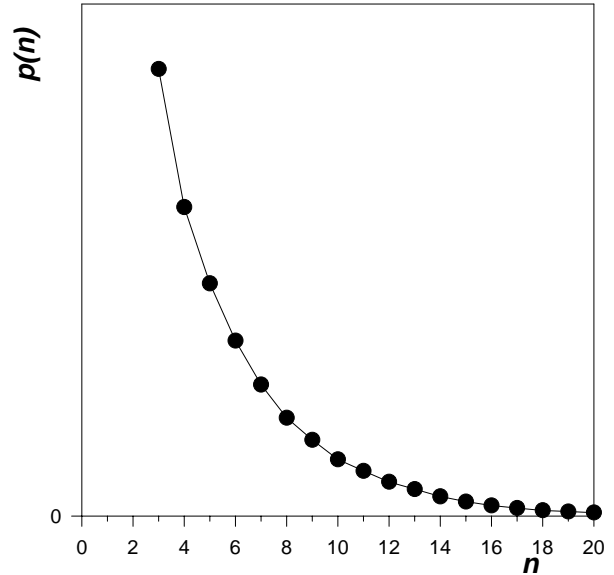

Fig. 8. Distribution of the number of edges per cell in the froth generated by T1 transformations (T1 simulation).

the system.) If the chosen edge is bounding a triangular cell, the T1 transformation is refused (lest it would generate a cell with two sides). The probability for a T1 to be refused increases during the disordering process, it reaches the value of 0.21 at the end of the simulation.

A typical cellular system obtained with this simulation is shown in Figure 2b. Figure 8 shows the probability distribution $p(n)$ for this froth. The second moment is $\mu_2 = 11.9$ and the Aboav-Weaire parameter is $a = -0.79$. The average number of sides per cell is equal to 6 (as imposed by the Euler theorem [2]) but the distribution is an exponential with a maximum at $n = 3$, $p(n) = p_3 \exp[-\alpha(n - 3)]$ with $p_3 = 0.27$ and $\alpha = 0.30$. In
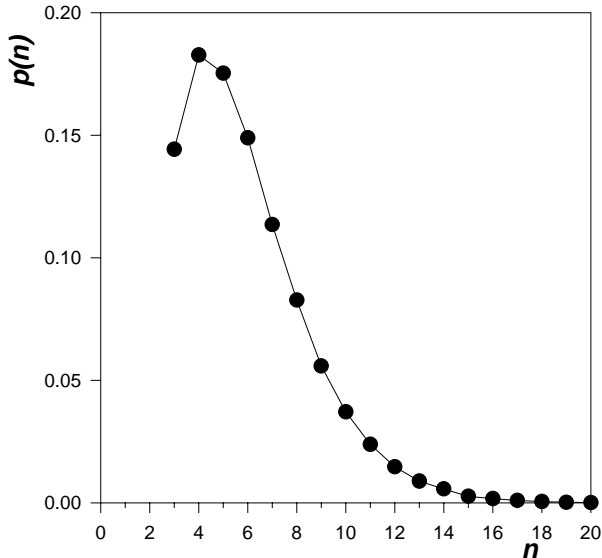
Fig. 9. Distribution of the number of edges per cell in the froth generated by T1 and T2 transformations (T1-T2 simulation).

Fig. 10. Two topologically equivalent views of the final configuration for the T1-T2 simulation. There are three cells of 6 sides tiling a torus. No further T1 or T2 transformations can be applied on this final, minimal configuration without generating a cell that is neighbour of itself.

this simulation, most of the cells are triangles because it is easier to generate a triangular cell than to make it gain an edge by random T1.

3.3 Random T1 and T2 (T1-T2 simulation)

In this type of simulation, a flip (T1 transformation) is performed on any edge chosen at random, except if the edge is bounding a triangular cell. In this case, the triangular cell is made to disappear (T2 transformation). For this reason, the number of cells decreases during the simulation. We found that, when $5N_0$ transformations are applied on an initially hexagonal lattice of N_0 cells, the number of cells is reduced by half. But $10N_0$ transformations are more than enough to reduce the froth to 3 (hexagonal) cells only. This is the minimum possible number of cells for a froth tiling a torus. Here each cell has 2 neighbours and 6 edges and they are arranged as shown in Figure 10. Note that, for this configuration, there are two families of closed paths of only 4 edges, not bounding a cell, that wind around the torus. No further T1 or T2 transformations can be applied on this final, minimal configuration without generating a cell that is neighbour of itself.

This simulation started with an hexagonal lattice of $N_0 = 250\,000$ cells on which we applied $5N_0$ of T1 or T2 transformations on edges chosen at random. The resulting structure had a number of cells $N = 115\,149$. A typical froth generated by T1-T2 transformations is shown in Figure 2c. The probability distribution $p(n)$ is plotted in Figure 9. It is quasi-stationary (until the system is close to its final configuration of 6 hexagonal cell). It has a maximum in $n = 4$ and then decreases with an exponential tail $p(n) = p_4 \exp[-\alpha(n-4)]$ with $p_4 = 0.84$ and $\alpha = 0.53$, for $n > 7$. The second moment is $\mu_2 = 6.33$ and the Aboav-Weaire parameter is $a = 0.05$.
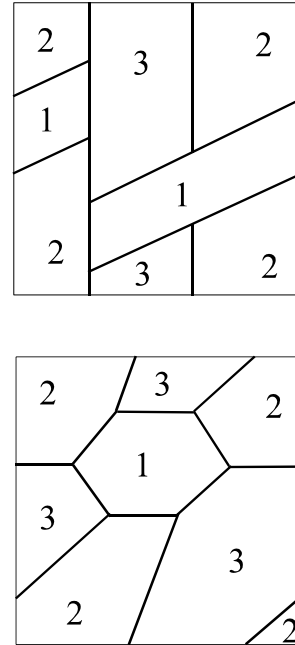
4 Results and discussion

For each simulation, the cellular systems are characterized by the number of cells in the shell structure (K_j), in the bond trees (F_t) and in the combined structure $(N(j,t))$, at the respective distances j and t of the central cell. The number of vertices in the bond trees V_t and their mean coordination z_t are also investigated.

4.1 Bond trees

The averaged number of cells in the bond tree $(\langle F_t \rangle = \sum_n p(n)F_t)$ as a function of the bond distance t is shown in Figure 11. For the three sets of simulations, $\langle F_t \rangle$ increases linearly with the distance as $t \to \infty$, with a slope 3.577 (D-C), 4.68 (T1) and 3.112 (T1-T2). As anticipated in Section 2, the number of vertices at distance t in the bond tree is expected to be proportional to the number of cells at that distance, $V_t = F_t/\nu_t$. Indeed, we find a coefficient of proportionality that asymptotically tends to $\nu_t \to \nu_\infty = 0.5$.

Asymptotically, the mean vertex connectivity z_t tends to 2, which is typical of a tree structure spanning vertices distributed uniformly on a finite area (see Figs. 3c and 12). There are n such trees for an n-sided central cell. If the trees were not impeding each other one would expect $V_t \propto tn$, asymptotically in t. But trees do impede each other. This interaction between the n trees implies that, after a certain distance, the leading contribution to V_t is proportional to t, regardless of n. The influence of the central cell is screened by the disorder [16], which distributes
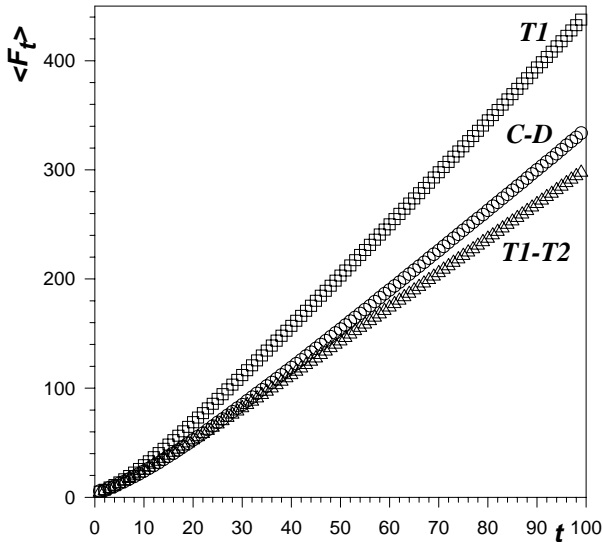
Fig. 11. Average number of cells $\langle F_t \rangle$ at distance t in the bond trees, for the three simulations C-D, T1 and T1-T2. The average is over all central cells.
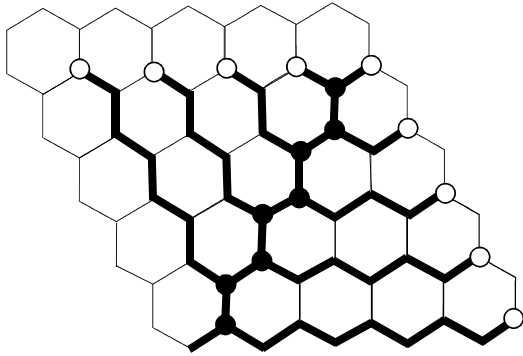

Fig. 13. Number of vertices V_t in the bond trees as function of the number of edges of the central cell n, for several bond distances t. The data refer to the C-D simulation. Similar behaviours were found for the other two types of simulations.

Fig. 12. A bond tree spanning $1 + t(t+1)/2$, uniformly distributed vertices (here on an hexagonal tiling). There are t vertices at distance t, at the end of the branches, with coordination 1 (white circles); the $t-1$ vertices on the main trunk have coordination 3 (black circles); the root has coordination 1. The remaining $1 + t(t-3)/2$ vertices have coordination 2. Thus $\langle z \rangle = 2 - O(1/t^2)$.

the vertices uniformly on the plane. This is manifest in Figure 13, which shows that V_t is linear in n, with a slope independent of t.

Fig. 14. Average number of cells $\langle K_j \rangle$ at distance j in the shell layers, for the three simulations C-D, T1 and T1-T2 and for the hexagonal lattice (($+$) symbol). The average is over all central cells.

4.2 Shell structures

The number of cells K_j at shell distance j (whether within layer (j) or inside defect inclusions) increases linearly with j after the first few layers. The dependence of K_j on the number of edges n of the central cell is also linear. Among all cells at distance j, the proportion belonging to defects is 18% for the C-D simulation, 52% and 38% for the T1 and T1-T2 simulations, stationary after a few layers. Figure 14 shows the averaged (over all central cells) number of cells $\langle K_j \rangle$ at a shell distance j. Figure 14 shows clearly
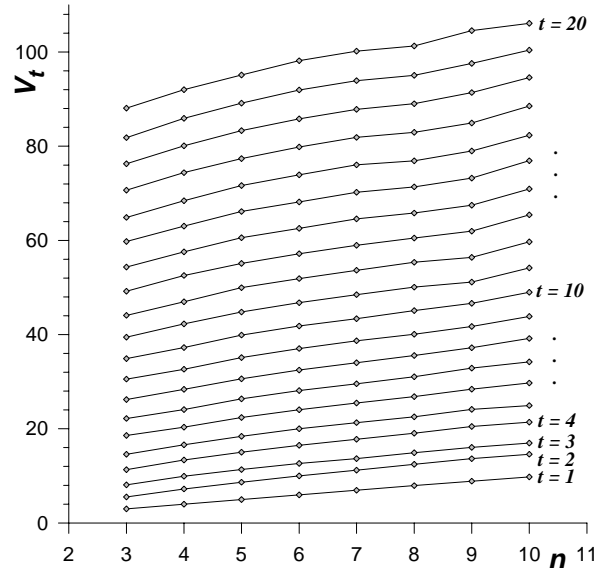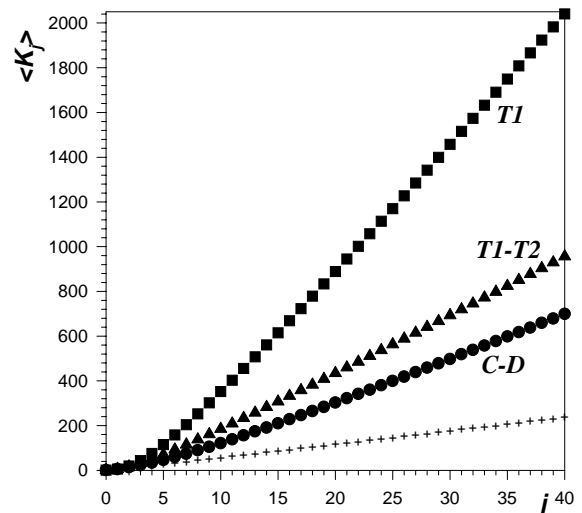
that the rate of growth C of $\langle K_j \rangle$ is very different in the three types of simulations. The number of cells at a given shell distance is larger in the more disordered systems. Specifically, the rate is $C = 19.35$ for the C-D simulation ($\mu_2 = 1.77$), $C = 56.6$ for the T1 simulation ($\mu_2 = 11.9$) and $C = 25.7$ for the T1-T2 simulation ($\mu_2 = 6.33$). These values are much larger than $C = 6$ for the hexagonal tiling ($\mu_2 = 0$), or than $C = 2\pi$ expected if layers were circular annuli. Indeed, in disordered froths the concentric layers wiggle around the averaged circular annulus.
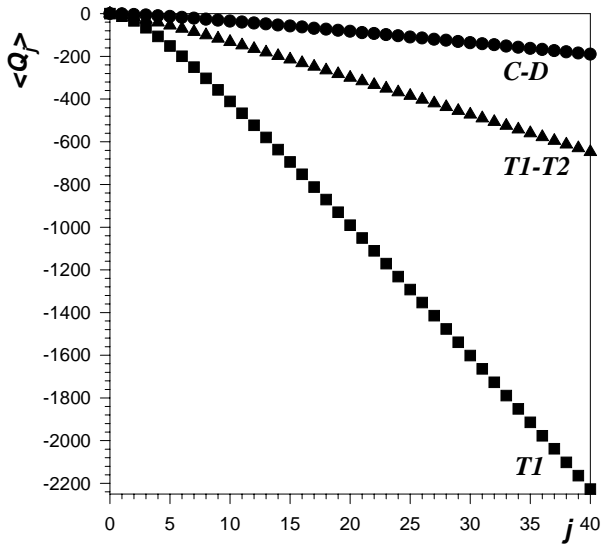
Fig. 15. Average topological charge $\langle Q_j \rangle$ *versus* j, within a cluster bounded by a layer of cells at shell distance j. The average is over all central cells. The topological charge of a n-sided cell is $6 - n$

Fig. 16. Number of couples of cells $N(j,t)$ at a shell distance j and bond distance t, as function of t for several values of j. The symbols are data taken from the T1 simulation. The full lines are the theoretical solution equation (2) with $\langle v \rangle = 1.39$. Note the linear correlation between the most probable value of t and j.

This behaviour has already been observed in soap and Voronoi froths [12]. It can be interpreted as an additional, negative curvature caused by the disorder, and compensated by the positive curvature of the defects intercalated between the layers to produce a tiling which is globally Euclidean. A relation for the slope C in froths free of topological defects (SSI) and with shortest ranged correlations was obtained in [12]: $C = 6 + (3 - a)\mu_2$, with a the Aboav-Weaire parameter. This relation gives $C = 10.2$, $C = 51.3$ and $C = 24.7$ for the C-D, T1 and T1-T2 simulations, respectively. The moderate agreement indicates that defects are relevant.

The topological charge (Q_j) of a cluster bounded by layer (j) (included) has been measured in the three types of simulation. Figure 15 shows the averaged charge $\langle Q_j \rangle$ as a function of the shell distance j (the average is over all the central cells). The topological charge $\langle Q_j \rangle$ is negative and decreases linearly with j (similar results were found for soap and Voronoi froths [12]). The mean topological charge per defect $\langle q^{\text{def}} \rangle$ is independent of j at large j. We found $\langle q^{\text{def}} \rangle = 1.1$ in the C-D simulation, $\langle q^{\text{def}} \rangle = 2.1$ and $\langle q^{\text{def}} \rangle = 1.8$ in the T1 and T1-T2 simulations, respectively.

The negative topological charge of the cluster (Q_j) is due to the wiggling of the boundary. The linearity shows that the amplitude of the wiggling remains constant with increasing shell distance. The boundary does not roughen as j increases. The negative charge of the cluster is balanced by the positive charges of the defects just outside its boundary.
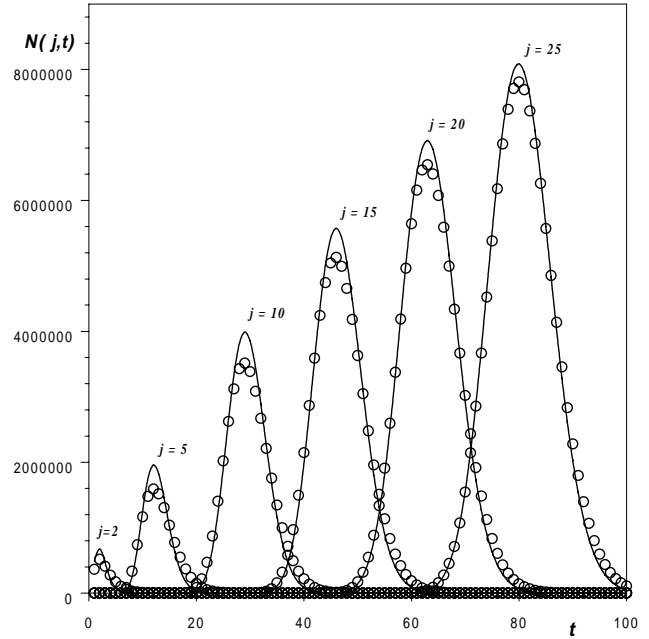
4.3 Combined structure

The distribution $N(j,t)$ of couples of cells at shell distance j and bond distance t is represented in Figure 16 as a function of t for different values of j, for the T1 simulations. Beyond $j = 10$, the distribution is symmetric, peaked at the mean value $\bar{t} = 3.39j - 4.2$, with a variance $\sigma^2 = 1.35j + 3.2$. The other two types of simulation exhibit similar behaviours. The theoretical distribution (a shifted Poissonian, Eq. (2), derived in Appendix A) is also plotted in Figure 16 (full line), with only one parameter $\langle v \rangle$ to be fitted ($\langle v \rangle$ measures the mean increase in lateral spread of the tree, due to disorder, it is defined in Sect. 2). The agreement is excellent. We obtain $\langle v \rangle = 0.31$ (C-D simulation), $\langle v \rangle = 1.39$ (T1 simulation) and $\langle v \rangle = 0.84$ (T1-T2 simulation). As expected, branches are longer in the more disordered systems.

5 Conclusions

We have simulated and analyzed very different cellular patterns which have only the name of froth in common: they are planar networks with minimal vertex connectivity. Several disordered froths with more than 10^5 cells were generated by computer simulations. The results presented in this paper refer to three types of simulations of cellular systems (C-D, T1 and T1-T2) generated with different techniques, which exhibit different degrees of disorder. They are summarized in Table 1. The T1 and T1-T2

Table 1. Summary of the results for the three simulations and the hexagonal tiling (see text).

	μ_2	a	slope $\langle F_t \rangle$	slope $\langle K_j \rangle$	$\langle v \rangle$
C-D	1.77	0.64	3.577	19.35	0.31
T1	11.9	-0.79	4.68	56.6	1.39
T1-T2	6.33	0.05	3.112	25.7	0.84
hexagonal tiling	0	-	0 (t even) 3 (t odd)	6	0

simulations generate very disordered systems where the number of edges of a cell fluctuates widely. (The sizes of the cells have not been relaxed or adjusted in our topological simulations). The C-D simulation generates a more homogeneous cellular pattern, somewhat akin to soap froths or other natural cellular structures. When C-D simulations are applied on an initially very disordered froth, the system self-organises, and a more homogeneous configuration with steady statistical properties is reached. In all three types of simulation, a stationary distribution of cells can be obtained. Moreover, the number of cells in the froth also remains stationary in the C-D simulation for a special value of the probability $p_d = 1/4$ of dividing 6-sided cells.

These disordered cellular structures were characterized in terms of two distances from an arbitrary central cell: the *bond* and the *shell* distance. In terms of bond distances, the froth is structured in a forest of n *bond trees*, rooted on the n vertices of the central cell. They have asymptotic vertex coordination $z_\infty = 2$ and the number of vertices V_t at a given distance t increases linearly both with n and with t.

The number of cells K_j at a shell distance j from a given central cell, increases linearly with j. This linearity seems to indicate that froths remain Euclidean structures, and that the concentric layers of cells at the same cell distance j from the central cell, if they wiggle, do not roughen. There is no indication of fractal behaviour in our simulations (see [17] for an — artificial — example of fractal froth). The rate of increase (C) of the number K_j of cells with the shell distance j varies strongly with the type of simulation. It is larger for the more disordered systems, $C = 6$ for the hexagonal tiling, and $C \simeq 19$, 25 and 56 for the C-D, T1-T2, and T1 simulations, respectively. The slope of K_j *versus* j is therefore a very good parameter to differentiate froths with various degrees of disorder. Moreover, these differences should be observable in the physical properties of the froth like the diffusion coefficient [18].

The topological charge Q_j of a cluster of cells at shell distances $i \leq j$ from a given central cell is negative, with a linear dependence on j. This shows that layers of equidistant cells wiggle without roughening at larger distances, that this negative topological charge or effective curvature is entirely due to the outermost layer, and that it is completely balanced by the positive charges of the topological defects just outside the outermost layer of the cluster.

In a given froth, the two topological structures *bond trees* and *shell structure* are intimately related. The combined structure was studied in terms of the number $N(j,t)$ of cells which are simultaneously at a shell distance j and at a bond distance t from a given central cell. We find that the combined structure is well described by only one parameter $\langle v \rangle$, the mean number of extra bonds between adjacent layers.

All two dimensional froths are topological cellular networks filling an Euclidean surface. Specific froths, whether natural or produced by different types of simulations, differ primarily by the amount of disorder, *i.e.* by the variance μ_2 of the distribution $p(n)$ of n-sided cells. Universality can be seen in the linear dependence of the number of cells K_j or F_t on the distance j or t and, independently, on n (the number of sides of the central cell). These are consequences of the flat surface on which the froth lies, regardless of the topological charge of the central cell [16]. Specificity shows up chiefly in the rate of increase (C) of the number K_j of cells at the same shell distance j (were $C - 6$ increases with μ_2). Disorder thickens the jth shell and wiggles its outer boundary. By contrast, the number F_t of cells at bond distance t is, asymptotically, uncorrelated to disorder. This is probably because the rooted bond trees impede each other.

Appendix A: Distribution of bond distances of cells all at the same shell distance

Here, we estimate the quantity $N(j,t)$. First consider the layer of cells at a shell distance j from the central cell. Let $P(t|j)$ be the conditional probability of finding, among all the cells at shell distance j from the central cell, a cell at a bond distance t. This probability can be written in terms of $N(j,t)$ as $P(t|j) = N(j,t)/[\sum_t N(j,t)]$. Let $w(i)$ be the probability to require $2+i$ bonds in the path between a layer and the next. Therefore, any cell in layer j is connected, in the bond tree, to a nearest cell the layer $j-1$ through a (shortest) path of $2+i$ bonds, with probability $w(i)$. Thus,

$$P(t|j) = \sum_{i=0}^{t-2j+3} w(i)P(t-i-2|j-1) \quad \text{(for } j > 2). \quad \text{(A.1)}$$

Let us now calculate $P(t|1)$ and $P(t|2)$. Cells sharing an edge with the central cell ($j = 1$) are at a bond distance zero. Thus, $P(t|1) = \delta_{t,0}$. Cells of the second layer ($j = 2$) are connected to the nearest cell in the first layer through a path of $1+i$ bonds with the same probability $w(i)$ ($i = 0$ labels those cells connected by one bond directly to the central cell). Thus,

$$P(t|2) = \sum_{i=0}^{t-1} w(i)P(t-i-1|1) = w(t-1). \quad \text{(A.2)}$$

This fixes the initial condition in equation (A.1).

The weights $w(i)$ can be in principle any discrete probability distribution. The simplest case is when $w(i) = \delta_{i,0}$. In this case, equation (A.1) has the solution $P(t|j) = \delta_{t,2j-3}$. This solution has values different from zero only for t odd, it corresponds to a structure with minimal bond length throughout, *i.e.* an hexagonal tiling, except for the arbitrary central cell.

A realistic probability function for the weights is the Poisson distribution of mean $\langle v \rangle$:

$$w(i) = \frac{\mathrm{e}^{-\langle v \rangle}\langle v \rangle^i}{i!} \,. \tag{A.3}$$

With this Ansatz, equation (A.1) has the solution

$$P(t|j) = \frac{\mathrm{e}^{-\langle v \rangle(j-1)}[\langle v \rangle(j-1)]^{t-2j+3}}{(t-2j+3)!} \,. \tag{A.4}$$

The number of couples of cells at shell distance j and bond distance t is $N(j,t) = NK_j P(j|t)$. As function of t (with j as a parameter) $N(j,t)$ is a shifted Poisson distribution with average $\bar{t} = \langle v \rangle(j-1) + 2j - 3$ and variance $\sigma^2 = \langle v \rangle(j-1))$.

References

1. D'A.W. Thompson, *On Growth and Form* (Cambridge, Univ. Press., 1917, 1942), chapter 7.
2. D. Weaire, N. Rivier, Contemp. Physics **25**, 59 (1984).
3. J. Stavans, Rep. Prog. Mod. Phys. **56**, 733 (1993).
4. J.W. Alexander, Ann. Math. **31**, 292 (1930).
5. B. Dubertret, N. Rivier, Biophys. J. **73**, 38 (1997).
6. B. Dubertret, *Études théoriques des systèmes cellulaires désordonnés. Application à la modélisation des tissus épithéliaux*, PhD Thesis (Université Louis Pasteur Strasbourg, France 1998).
7. B. Dubertret, K.Y. Szeto, W.Y. Tam, in preparation (1997).
8. N. Rivier, unpublished notes (1985); seminar, Imperial College (1986).
9. J.P. Troadec, unpublished notes (1985).
10. M.A. Fortes, P. Pina, Philos. Mag. B **67**, 263 (1993).
11. T. Aste, D. Boose, N. Rivier, Phys. Rev. E **53**, 6181 (1996).
12. T. Aste, K.Y. Szeto, W.Y. Tam, Phys. Rev. E **54**, 5482 (1996).
13. T. Aste, N. Rivier, in *Shape Modelling and Applications* (IEEE Computer Society Press, 1997), pp. 2-9.
14. D.A. Aboav, Metalloraphy **3**, 383 (1974); *ibid.* **13**, 43 (1980).
15. D. Weaire, Metallography **7**, 157 (1974).
16. N. Rivier, B. Dubertret, T. Aste, H.M. Ohlenbusch, in preparation (1997).
17. R. Delannay, G. LeCaër, J. Phys. I France **5**, 1417 (1995).
18. T. Aste, Phys. Rev. E **55**, 6233 (1997).